Application of Potential Based Cohesive Model for Analysis of Concrete Fracture

Habtamu A. Tadesse[1(✉)], Temesgen Wondimu Aure[2], and Alemayehu Golla Gualu[1]

[1] Faculty of Civil and Water Resources Engineering, Bahir Dar Institute of Technology, Bahir Dar University, Bahir Dar, Ethiopia
[2] College of Architectural and Civil Engineering, Addis Ababa Science and Technology University, Addis Ababa, Ethiopia
temesgen.wondimu@aastu.edu.et

Abstract. Concrete is the main construction material used for infrastructure construction around the globe. Since it is a brittle material, applied loads on concrete structures will result in sudden failure of the structure, and consequently the service of the structure will be affected. To prevent such failure, it is necessary to understand and predict the behavior and failure mechanics of concrete. Recently, the concept of the cohesive zone model has been widely applied to investigate various material failure phenomena. The potential-based model has advantages over the non-potential-based cohesive model in that their traction-separation relations are determined by taking the derivative of potential (cohesive interaction) concerning normal and tangential opening displacements. The purpose of this study is to evaluate the application of potential-based cohesive model for the study of concrete fracture by employing a user element in ABAQUS. The simulation is compared with reproduced experimental results and good agreement has been found between load-displacement curves.

Keywords: Cohesive model · Potential based model · Concrete fracture · Fracture mechanics

1 Introduction

Fracture of construction materials has been a problem since the construction of man-made structures has started. Nowadays the problem actually has become worse than in the previous centuries because of the spread of advanced and technologically complex construction. One of the most important aspects of fracture mechanics is to identify the potential dangers whenever the structural complexity is increased (Anderson et al. 1971).

The application of fracture mechanics into concrete has helped to achieve uniform safety margins and/or reliability. Fracture mechanics can help to understand the failure of high strength concrete structures and concrete structures of unusually large sizes. It has been discovered that many failures have been caused by pre-existing flaws in materials that initiate cracks that grow and finally lead to fracture.

M. L. Berihun (Ed.): ICAST 2021, LNICST 412, pp. 15–26, 2022.
https://doi.org/10.1007/978-3-030-93712-6_2

The collapse and failure of these infrastructures result in significant accidents, life loss, and damaging property and highly influence the local economy. To prevent such disasters, it is necessary to understand and predict the deformation and failure mechanisms of concrete (Park 2009).

Previous studies have indicated that a two-dimensional cohesive model was implemented in commercial software ABAQUS for different materials. However, the built-in traction separation relations for cohesive elements in commercial software have limitations since the tangent stiffness under the softening condition for the traction-separation relationship leads to non-physical responses. This limitation can be solved by providing a user element in ABAQUS. The user element (UEL) has been developed based on potential-based cohesive elements proposed by Park et al. (2009). However, the application of these elements for concrete fracture has not been examined.

The objective of this study is to implement a potential-based cohesive model for concrete fracture using UEL subroutine in commercial software ABAQUS. That means crack propagation phenomena is investigated through the potential based constitutive model in association with robust and efficient computational method.

More specifically, this study addresses with comparing analytical solutions and numerical simulation results by varying physical macroscopic fracture parameters, such as the shape of softening curve.

2 Methodology

The general purpose finite element software ABAQUS and analytical computations are used to investigate crack propagation phenomena of concrete through the user-defined element subroutine of ABAQUS. The user element subroutine of the ABAQUS code is written in FORTRAN. There are two approaches for inserting a cohesive element into the mesh. One way is either inserting the cohesive element along the pre-selected fracture path, by restricting the crack propagate where the user has specified or another way is by inserting it between all bulk elements in a region of mesh, allowing the fracture to propagate freely within that region (Daniel and Glaucio 2014).

The goals of this study will be achieved through the potential-based cohesive model first proposed by Park et al (PPR) (2009) in conjunction with robust and effective computational methods as the first step. The PPR model is a function of four basic independent parameters in the normal and shearing fracture modes, namely cohesive strength, fracture energy, the shape of softening curve, and the initial slope of the traction–separation relationship. The potential (for 3D in general), ψ, is given by (Park and Paulino 2012)

$$\Psi(\Delta n, \Delta t1, \Delta t2) = \min(\phi n, \phi t) + \left[\Gamma' n\left(1 - \frac{\Delta n}{\delta n}\right)^{\alpha}\left(\frac{m}{\alpha} + \frac{\Delta n}{\delta n}\right)^{m} + (\phi n - \phi t)\right]$$
$$* \left[\Gamma' t\left(1 - \frac{\sqrt{(\Delta t1)^2 + (\Delta t2)^2}}{\delta t}\right)^{\beta}\left(\frac{n}{\beta} + \frac{\sqrt{(\Delta t1)^2 + (\Delta t2)^2}}{\delta t}\right)^{n} + (\phi t - \phi n)\right] \tag{1}$$

Numerical simulation of mixed-mode fracture is implemented in commercial software ABAQUS with a user element subroutine. The rectangular plane stress element (Q4) is used for the bulk element, while the cohesive surface element is inserted along the crack path.

The rationale behind using this model is that the post peak behavior is captured well using different parameters with the most powerful function called *Potential Function*. A two dimensional simulations has been used by assuming a unit thickness to minimize the computation time.

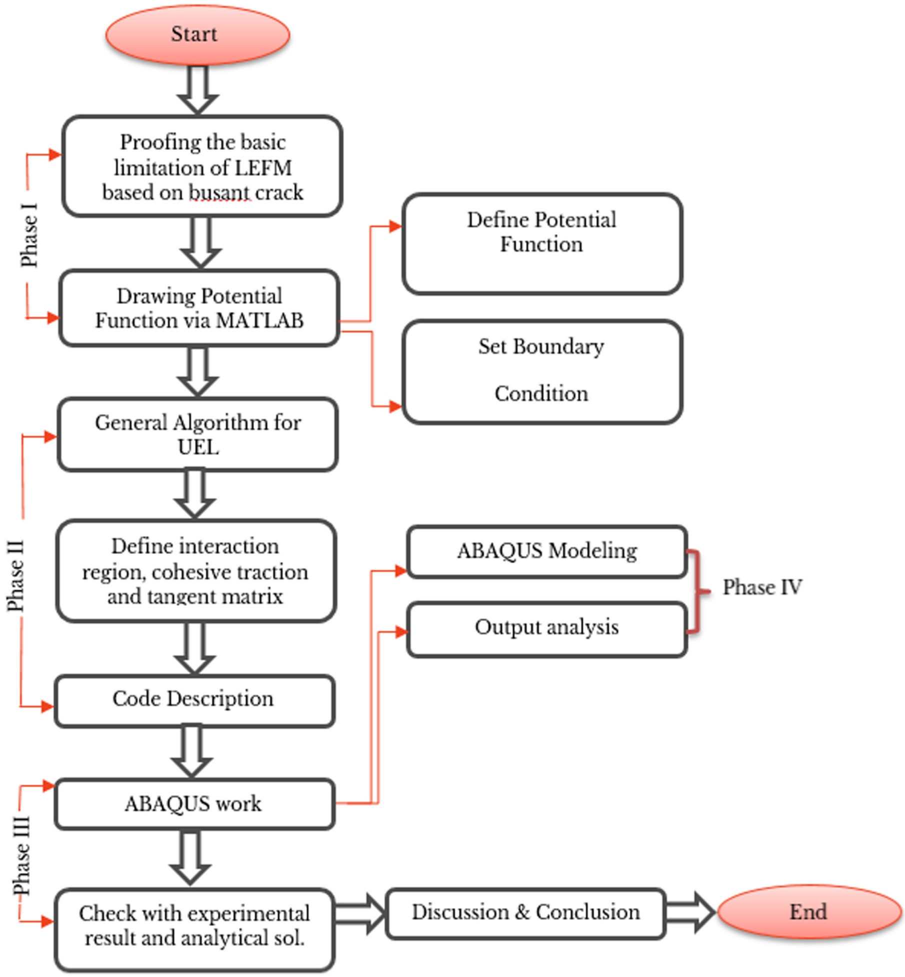

Fig. 1. Flow chart

The flow chart show in Fig. 1 illustrates the basic steps that have been followed to implement the user element. The procedure starts with receiving nine input data including thickness of a cohesive element. Those global coordinates are changed to local coordinates. Next, normal and tangential cohesive traction are computed. Finally, the cohesive interaction is defined in four chapters is Contact formulation, softening condition, unloading/Reloading condition, and complete failure (Fig. 2).

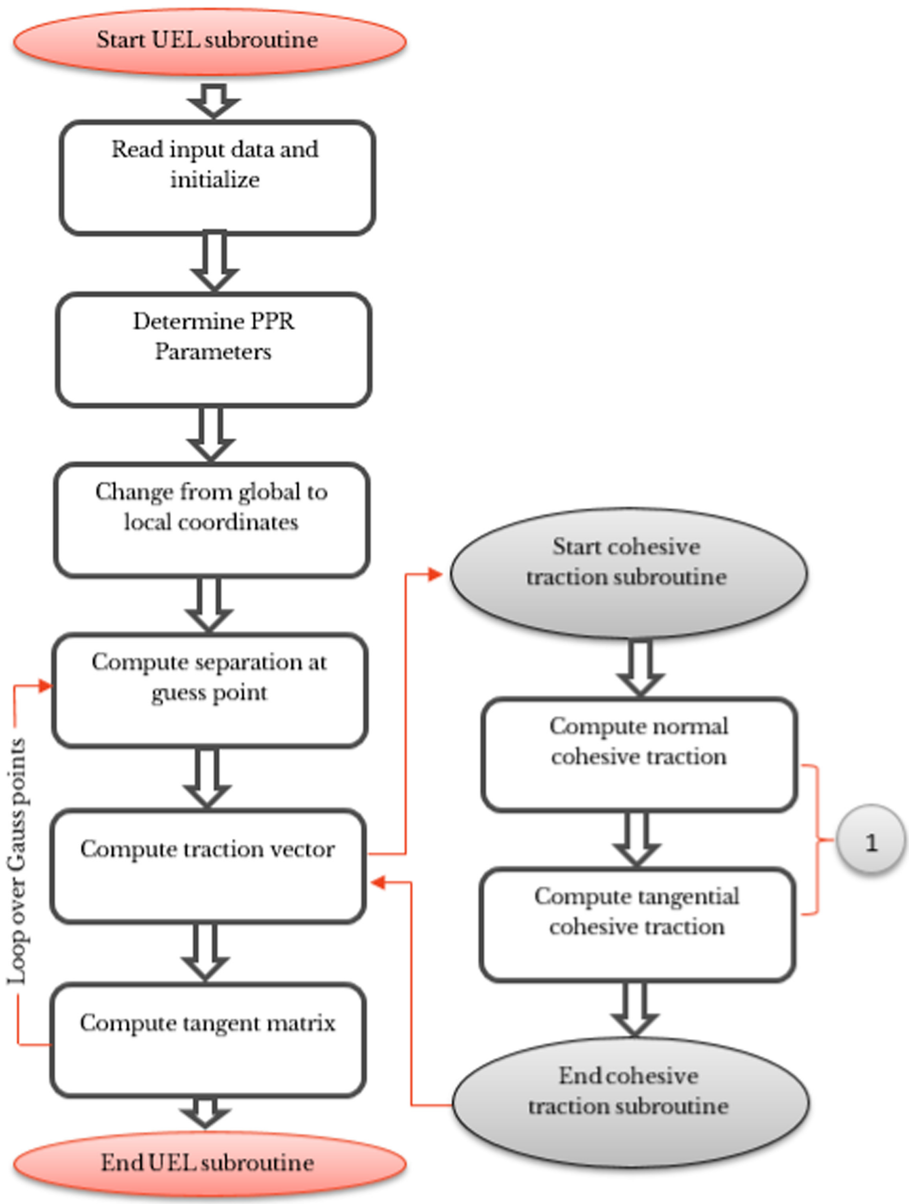

Fig. 2. General flow chart for UEL

2.1 PPR Implementation in ABAQUS

To alleviate any confusions between the code and this paper is the description in detail (Table 1 and Fig. 3):

Table 1. PPR UEL nomenclature and description

Paper	Fortran	Description
Bc	Bc	global displacement-separation relation matrix
$f\,coh$	Fc	internal force vector of a cohesive surface element
$Kcoh$	Sc	tangent matrix of a cohesive surface element
m, n	m, n	Non-dimensional exponents in the PPR model
N	ShapeN	shape functional matrix
Tc	T	cohesive traction vector
u	U	displacement field
U	U_l	nodal displacement vector in the local coordinates
α, β	alph, beta	shape parameters in the PPR model
$\Gamma n, \Gamma t$	Gam_n, Gam_t	energy constants in the PPR model
$\delta n, \delta t$	dn, dt	normal and tangential final crack opening widths
$\Delta nmax, \Delta tmax$	deln_max, delt_max	maximum normal and tangential separations in the loading history
$\lambda n, \lambda t$	ln, lt	initial slope indicators in the PPR model
Λ	R	coordinate transformation matrix
$\sigma max, \tau max$	Tn_m, Tt_m	normal and tangential cohesive strengths
$\varphi n, \varphi t$	Gn, Gt	normal and tangential fracture energies

3 Results and Discussion

3.1 Validation of the PPR Model

To validate the PPR model for quasi-brittle materials (like concrete), numerical simulation results are compared with reproduced experimental results from the three-point bending test of plain concrete (Roesler et al. 2007), shown in Fig. 4. The cohesive element size is taken to be 1 mm which is small enough to capture the local fracture process (Tables 2 and 3).

Table 2. Hardened properties of the concrete

Modulus of elasticity (GPa)	32
Compressive strength (MPa)	58.3
Poisson's ratio	0.2

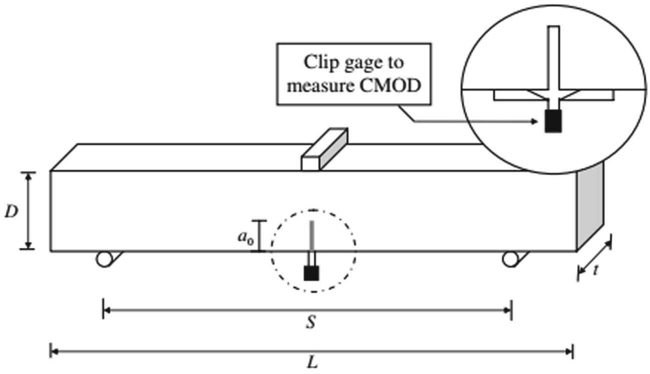

Fig. 3. Specimen dimensions and test configuration (Roesler et al. 2007)

Table 3. Specimen geometry of three-point test according to Roesler et al. (2007) experiment

	Specimen dimensions (mm)				
Beam Specimen ID	Length (L)	Depth (D)	Thickness (t)	Notch (a_o)	Span (S)
B150-80	700	150	80	50	600

It has an initial notch (ao) of 50 mm and a length of 700 mm. The simply supported beam mesh detail around the crack tip is shown in Fig. 4.

The finite element model of the beam is shown below which is created by the 2D planar option. The following beam has 150 mm depth and 700 mm length. The notch depth was taken to be 50 mm (Fig. 5).

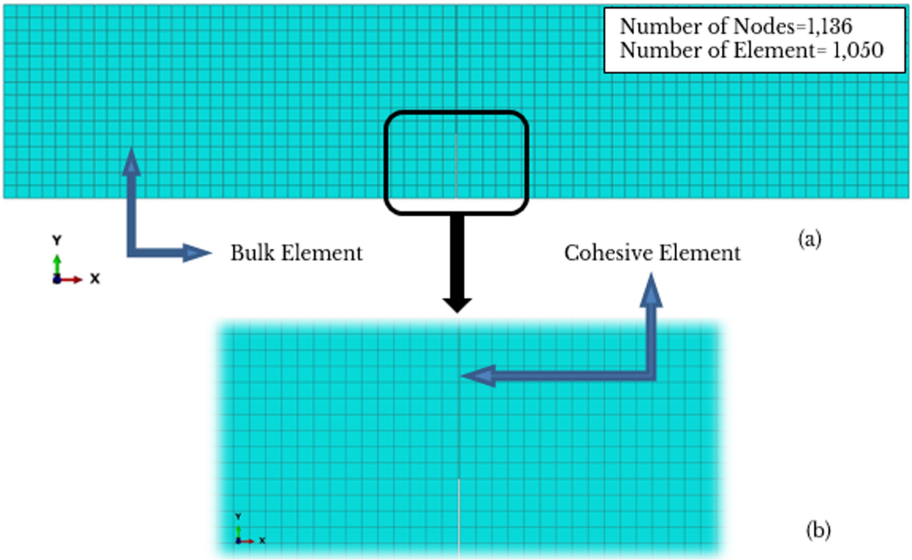

Fig. 4. 2D planar model mesh around the notch (b)

The following two-dimensional planar simply supported beams have been analyzed in ABAQUS UEL configuration. Since this research is concerned with mode I fracture, the crack is assumed to be propagated on a straight line in the vertical direction. As a result, ABAQUS ODB file indicated the following damage (Fig. 6) propagation for 10 stepwise increments with a 0.01 mm/s loading rate. The post peak behavior and the evolution of crack is independent of loading rate and thus taking this rate will be fair enough. The support assumed to carry vertical load only (roller support). The figure shows the stress distribution at the stated stage. Since the stress distribution shows maximum values at the loading points, which are expected locations to attract maximum effect at an early stage of loading, the numerical analysis result will be convenient.

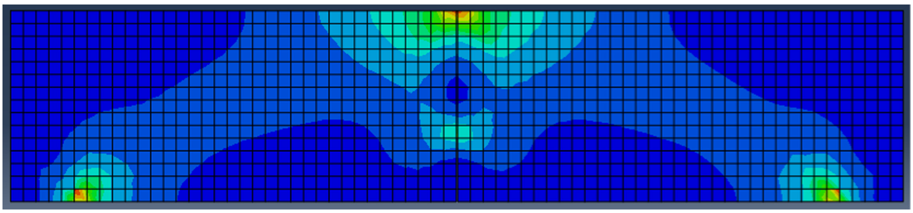

Fig. 5. Damage level from initial loading

At the final step of loading rate the cohesive element sweep in a vertical direction as shown in the figure below. The connectivity of elements has been assured by equal mesh size between the bulk element and cohesive element (Fig. 7).

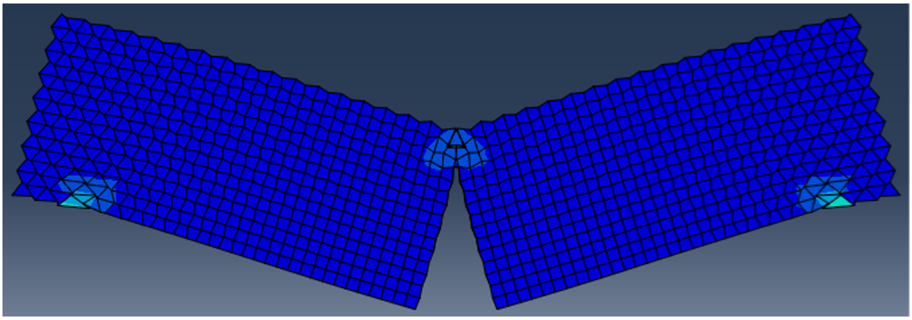

Fig. 6. Damage level from initial loading to final

3.2 Effect of Shape Parameters

The effect of shape values for numerical analysis has been investigated. The load-displacement relationship in Fig. 8 illustrates different α values under the same load control while other parameters were maintained. Initially, the load-displacement relationship of the analysis result has shown linear and similar behavior for different α values with slightly different behavior near to peak loads. However, in the post-peak region, the relationship of load-displacement for different α values has shown different behavior. As it can be seen from the graph, the experimental and the numerical analysis result has shown a good agreement when the value of α becomes greater than two.

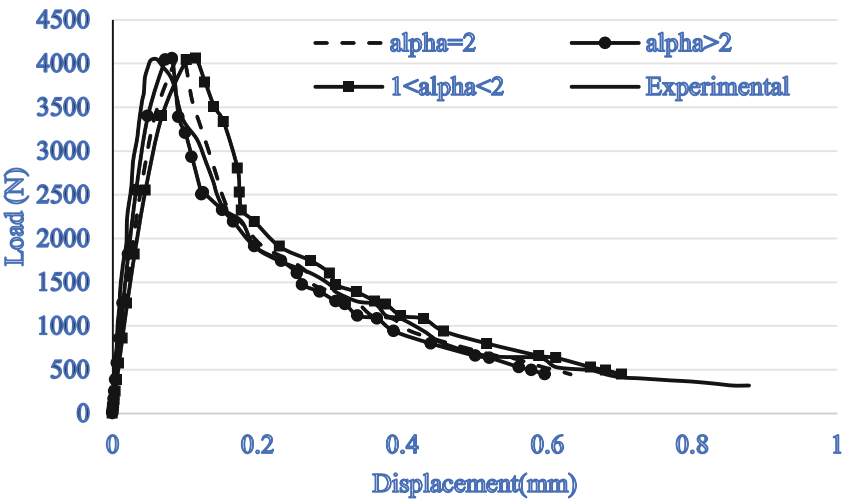

Fig. 7. Load vs displacement curve for different shape values (α = 1.5, 2, 5)

Based on the comparison between numerical and experimental values for peak load, the error has found to be 1.7%. Since the error is insignificant, this shows that the numerical simulation in ABAQUS UEL is acceptable.

3.3 Effect of Fracture Energy

The change in α value on potential function will also affect fracture energy. For each of the following cases, the fracture energy is calculated according to the PPR polynomial function. The area under the cohesive interactions corresponds to fracture energy:

$$\emptyset_n = \int_0^{\delta n} Tn(\Delta n, 0) d\Delta n \quad (2)$$

The following normal traction curve is generated from Matlab GUIDE which indicates the value of fracture energy at the atomistic level.

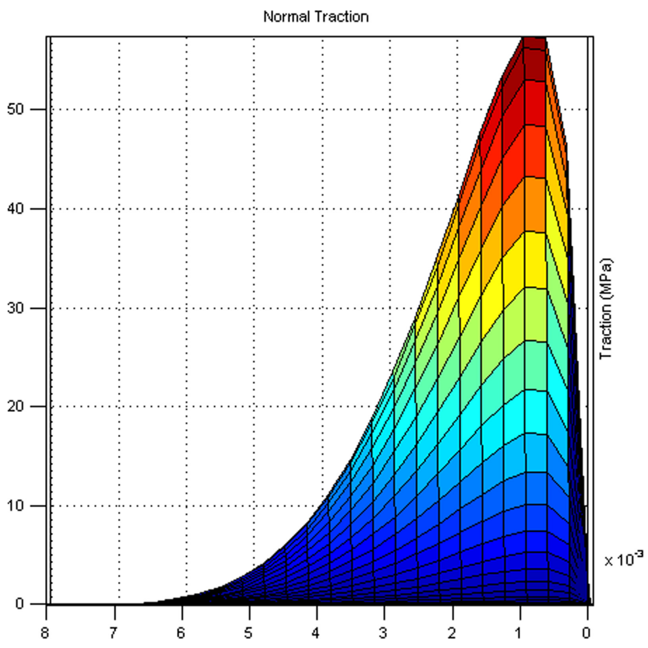

Fig. 8. Normal traction curve for alpha = 5

The normal traction Tn is expressed as:

$$T_n(\Delta n, \Delta t) = \frac{\acute{\Gamma} n}{\delta n}\left[m\left(1-\frac{\Delta n}{\delta n}\right)^{\alpha}\left(\frac{m}{\alpha}+\frac{\Delta n}{\delta n}\right)^{m-1} - \alpha\left(1-\frac{\Delta n}{\delta n}\right)^{\alpha-1}\left(\frac{m}{\alpha}+\frac{\Delta n}{\delta n}\right)^{m}\right] * \left[\acute{\Gamma} t\left(1-\frac{\Delta t}{\delta t}\right)^{\beta}\left(\frac{n}{\beta}+\frac{\Delta t}{\delta t}\right)^{n} + \langle \phi t - \phi n\rangle\right] \tag{3}$$

Although the two-dimensional potential model captures fracture behavior by changing the softening curve, the models do not have the same fracture energy in modes I and II (Fig. 9).

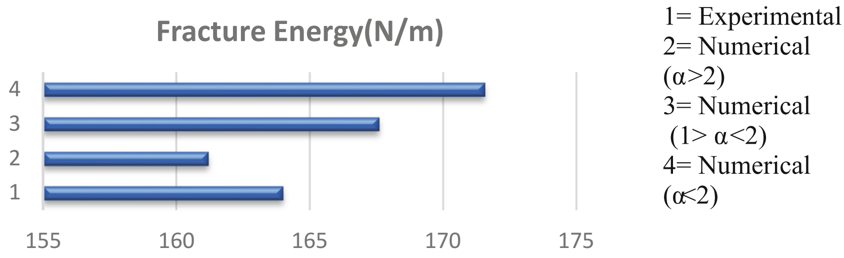

Fig. 9. Fracture energy comparison between numerical and experimental simulation

The above figure shows the fracture energy value of the experimental result and numerical analysis results with different alpha (α) values. When it has compared between numerical and experimental values of fracture energy with alpha equal to 5, the error has found to be 1.52%. This error is also insignificant like the load-displacement relationship error found with experiment and analysis results. This can have confirmed that ABAQUS can simulate the real post-peak behavior of concrete in the PPR model.

4 Conclusion

From the analysis results, it has been found that there is good agreement between the load-displacement curve obtained from the experiment and numerical simulation. And the shape factor is the most determinant factor in the PPR model. So far polynomial PPR function that represents the best fit for numerical simulation in softening curves is α = 5. Again the maximum load has also a good agreement between the two simulations. The good agreement between alpha value and compressive strength are not related directly or inversely.

For α greater than two, the cohesive traction separation relationship has a convex shape, which can be utilized for plain concrete.

It should be noted that one of the key contributions of this research is to link the experimental fracture properties with the numerical fracture properties with PPR and implement into finite element in UEL subroutine to predict crack propagation and behavior. In addition to this, the evolution of crack is related with critical stress of the crack tips. Whenever the stress at initial crack is critical, the micro crack will created by connecting another element which reached with critical stress.

References

Anderson, G.P., Ruggles, V.L., Stibor, G.S.: Use of finite element computer programs in fracture mechanics. Int. J. Fract. Mech. **7**(1), 63–76 (1971)

Anderson, T.L.: Fracture Mechanics: Fundamentals and Applications. CRC Press (1995)

Anderson, T.: Fracture Mechanics Fundamentals and Application. London (2005)

Andrew, J.: A Descriptive Analysis of Stadiums as Non-sporting Event Values (2017)

ASTM. Standard Test Method for Mixed Mode-I Mode II Interlaminar Fracture Toughness of Unidirectional Fiber Reinforced Polymer Matrix Composites. ASTM D 6671/D 6671M. ASTM International (2006)

Banks-Sills, L., Bortman, Y.: A mixed-mode fracture specimen: analysis and testing. Int. J. Fract. **30**(3), 181–201 (1986)

Barenblatt, G.I.: The formation of equilibrium cracks during brittle fracture. General ideas and hypotheses. Axially-symmetric cracks. J. Appl. Math. Mech. **23**(3), 622–636 (1959)

Barker, R.M., Puckett, J.A.: Design of Highway Bridges: An LRFD Approach, 2nd edn. Wiley, New York (2007)

Bazant, Z.: Fracture and Size Effect in Concrete and Other Quasi-Brittle Material. Madrid (1997)

Bažant, Z.P., Becq-Giraudon, E.: Statistical prediction of fracture parameters of concrete and implications for choice of testing standard. Cem. Concr. Res. **32**(4), 529–556 (2002)

Bažant, Z.P., Caner, F.C.: Microplane model M5 with kinematic and static constraints for concrete fracture and anelasticity. I: Theory. J. Eng. Mech. **131**(1), 31–40 (2005)

Bažant, Z.P., Caner, F.C., Carol, I., Adley, M.D., Akers, S.A.: Microplane model M4 for concrete. I: formulation with work-conjugate deviatoric stress. J. Eng. Mech. **126**(9), 944–953 (2000)

Bazant, Z.P., Planas, J.: Fracture and Size Effect in Concrete and Other Quasibrittle Materials. CRC Press (1998)

Beltz, G.E., Rice, J.R.: Dislocation nucleation versus cleavage decohesion. In: The Minerals, Metals & Materials Society (TMS), pp. 457–480 (1991)

Borsi. Advanced Mechanics of Material (2002)

CEO, A.: Getting Started with Abaqus_Standard Manual (2012)

Cornec, A., Scheider, I., Schwalbe, K.-H.: On the practical application of the cohesive model. Eng. Fract. Mech. **70**(14), 1963–1987 (2003)

Daniel, W.S., Glaucio, H.P.: A growing library of three dimensional cohesive elements for use in ABAQUS. Eng. Fract. Mech. (2014)

Falk, M., Needleman, A.: A Critical Evaluation of Cohesive Zone Models of Dynamic Fracture, vol. 11. Netherlands (2001)

Hillerborg, A., Modéer, M., Petersson, P.-E.: Analysis of crack formation and crack growth in concrete by means of fracture mechanics and finite elements. Cem. Concr. Res. **6**(6), 773–782 (1976)

Hutchinson, V.T.: The influence of plasticity on mixed mode interface toughness. J. Mech. Phys. Solids **41**(6), 1119–1135 (1993)

Ingraffea, A.R., Gerstk, W.H., Gergely, P., Saouma, V.: Fracture mechanics of bond in reinforced concrete. J. Struct.. Eng. **110**(4), 871–890 (1984)

Jorg, F.U., Stafen, E., Carsten, K.: Modelling of cohesive crack growth in concrete structures with extended finite element method. Comput. Method. Appl. Mech. Eng. (2007)

Needleman, A.: A continuum model for void nucleation by inclusion debonding. J. Appl. Mech. **54**(3), 525–531 (1987)

Needleman, A.: An analysis of tensile decohesion along an interface. J. Mech. Phys. Solids **38** (3), 289–324 (1990)

Needleman, A., Tvergaard, V.: An analysis of ductile rupture in notched bars. J. Mech. Phys. Solids **32**(6), 461–490 (1984)

Park, K.: Concrete Fracture Mechanics and Size Effect. Illinois (2003)

Park, K.: Potential Based Fracture Mechanics Using Cohesive Zone and Virtual Internal Bond Modeling. University of Illinois, Urbana, Illinois (2009)

Park, K., Paulino, G.H.: Computational implementation of the PPR potential-based cohesive model in ABAQUS: educational perspective. Eng. Fract. Mech. **93**, 239–262 (2012)

Park, K., Paulino, G.H., Roesler, J.R.: Determination of the kink point in the bilinear softening model for concrete. Eng. Fract. Mech. **75**(13), 3806–3818 (2008)

Park, K., Paulino, G.H., Roesler, J.R.: A unified potential-based cohesive model of mixed-mode fracture. J. Mech. Phys. Solids **57**(6), 891–908 (2009)

Park, K., Pereira, J.P., Duarte, C.A., Paulino, G.H.: Integration of singular enrichment functions in the generalized/extended finite element method for three dimensional problems. Int. J. Numeric. Method. Eng. **78**(10), 1220–1257 (2009)

Park, K., Paulino, G.H.: Cohesive Zone Model: A Critical Review of Traction-Separation Relationship Across Fracure Surfaces. Trans. ASME (2014)

Parks, M.L., Lehoucq, R.B., Plimpton, S.J., Silling, S.A.: Implementing peridynamics within a molecular dynamics code. Comput. Phys. Commun. **179**(11), 777–783 (2008)

Paulino, G.H., Menezes, I.F.M., Cavalcante Neto, J.B., Martha, L.F.: A methodology for adaptive finite element analysis: towards an integrated computational environment. Comput. Mech. **23**(5–6), 361–388 (1999)

Perez, N.: Fracture Mechanics. London (2004)

Roesler, J., Paulino, G.H., Park, K., Gaedicke, C.: Concrete fracture prediction using bilinear softening. Cem. Concr. Compos. **29**(4), 300–312 (2007)

Rosa, A.L., Yu, R.C., Ruiz, G., Saucedo, L., Sousa, J.L.: A loading rate dependent cohesive model for concrete fracture. Eng. Fract. Mech. (2011)

Uday, N.P.: Experimental determination of fracture energy by RILEM method. Int. J. Eng. Sci. **06**(03), 106–115 (2017)

Xu, X.-P., Needleman, A.: Void nucleation by inclusion debonding in a crystal matrix. Model. Simulat. Mater. Sci. Eng. **1**(2), 111–132 (1993)

Xu, X.-P., Needleman, A.: Numerical simulations of fast crack growth in brittle solids. J. Mech. Phys. Solids **42**(9), 1397–1434 (1994)